JJMIE

Volume 18, Number 2, June. 2024
ISSN 1995-6665
Pages 391- 400
https://doi.org/10.59038/jjmie/180211
Editor-in-Chief: Prof. Ali M. Jawarneh

Jordan Journal of Mechanical and Industrial Engineering

Control Degradation of New Magnesium Alloy by MgF2 Coating for Cardiovascular Applications

Baraa H. Al khaqani* , Nawal Mohammed Dawood

College of Materials Engineering, University of Babylon, Iraq

Received 16 Jul 2023 *Accepted 24 Mar 2024*

Abstract

The deployment of permanent biomaterials has significantly modified in the last few decades. Magnesium (Mg) and its alloys' inherent ability to break down without producing harmful products has opened up a wide range of biomedical applications, including musculoskeletal, orthopedic, and cardiovascular stent applications. This work investigated the control of the degradation rate and also improved the corrosion resistance of novel magnesium biodegradable alloy via fluoride chemical conversion coating. However, the surface roughness, corrosion resistance, and degradation rate of the chemical conversion film (MgF_2) with various physiological solutions have been investigated in this study. We established the rules that the MgF_2 film with a greater thickness of 14.21µm and better corrosion resistance were produced under longer preparation times through in vitro hydrogen evolution volume 0.037 ml/cm^2 change P.H. of solutions, composition and structure analysis, and roughness of surface 27.8 nm. Comparing the variations of various classification techniques, addition of the MgF_2 film can have high bonding strength with substrate greater than 50 MPa as the corrosion rate with PDP reduced from 3.37 mm/y to 0.62mm/y for Alloy with coating MgF_2 in simulated blood plasma, respectively while decreasing the corrosion rate in phosphate buffer saline from 17.07 mm/y to 1.55 mm/y. At the same time, we showed that the MgF_2 film was highly cytocompatible and that osteoblasts attached to and formed satisfactorily on its surface. These findings significantly affect how the MgF_2 film is used in cardiac stents.

Keywords: Mg-Biodegradable Alloys, Surface Modification, Fluorite Chemical Conversion, Degradation Rate.

1. Introduction

Metallic materials with good corrosion resistance and long-term structural stability, like stainless steel, Co-Cr alloys, and Ti alloys, are helpful in applications in medicine [1, 2]. However, excessive intercellular corroding of nanomaterials may cause allergic or inflammatory responses, which lowers their biocompatibility[3,33,34]. However, removing implants after a fracture heals, increases patient pain and expenses of care. A further significant disadvantage of internal fixations is stress shielding, which hinders bone growth and decreases the strength of new bone [4,35,36]. Thus, removing the internal suture might result in a second fracture due to its insoluble nature in bodily fluids; fluoride coating can protect the magnesium surface [5]. The initial reference to the development of degradable alloys based on magnesium can be found in the paper on who managed bleeding valves with magnesium wire ligatures. Many modern investigations have documented the development of coating treatment on healthcare magnesium alloys [6], emphasizing the enhancement of durability to corrosion as well as the multifunctional properties of adaption, bioactivity, and biodegradability in addition to biocompatibility. This study seeks to provide, from methodical, structural, and functional angles, the state-of-the-art developments and scientific concerns surrounding coatings on magnesium alloys during the past ten years. On magnesium alloys, coats can be applied mechanically, physically, chemically, biologically, or bio mimetically [7]. The coverings' layout and specifics ,are shown in Figure 1.

1. Shot peening, friction, and wear can be used to create mechanical coatings.
2. Magnetic sputter laser cladding, an electron beam, and ion implantation methods create physical coats.
3. Chemically conversion, electro-deposition, sol-gel, electro less plating, micro-arc oxidation (MAO) or plasma electrolyte oxidation (PEO), layer-by-layer assemblage, and ionizing liquids are methods used to create biochemical coats.
4. The recognition of molecules and bio-mineralization are two aspects of biomedical approaches.

Yan et al.in 2014 [9] have revealed how the fluorite layer may improve the AZ31B alloy's surface biocompatibility and durability against corrosion. Their research also showed the coating's antibacterial properties.Sun et al. in 2019 [10] Founded that coating Mg surfaces with ultrasonic cleaner speeds up the rate of color change in earlier fluoride conversion coating experiments. Based on this research, we

* Corresponding author e-mail: baraaalkhaqani@gmail.com.

hypothesize that when compared with fluoride conversion-coated Mg and bare Mg, the corrosion durability of fluoride conversion-coated Mg can be further enhanced with the use of ultrasonic treatment; the results showed that the film thickness after 24-h/48-h/96-h treatment was about three μm, 3.5 μm, four μm. It can be seen that there is a positive correlation between film thickness and immersion time, but the scale difference is not too large. According to electrochemical studies, the corrosion resistance of magnesium alloys in SBF is significantly improved by forming a fluoride film. Magnesium alloys with a fluoride treatment have been concluded to have a low degradation rate and excellent biocompatibility in vivo studies using animal models[8,37]. The fluoride conversion coating has enhanced the corrosion resilience of magnesium; however, it has yet to be used in medical applications; author found that coating Mg surfaces with an ultrasonic cleaner speeds up the rate of color change in earlier fluoride conversion coating experiments. Based on this research, the corrosion durability of fluoride conversion-coated Mg can be further enhanced with ultrasonic treatment when compared with fluoride conversion-coated Mg and bare Mg [1]. Recent developments have made fluoride treatment possible for preparing the protective chemical fluoride conversion coating (MgF_2) for significant Mg alloy corrosion protection due to intense chemical adhesion on the substrate. The author observed that fluorine treatment could cut the corrosion rate of WE43 Mg alloy in half by using fluoride treatment[8]. The Authors formed a uniform fluoride conversion coating that improved the corrosion endurance of the Mg-3Zn-0.5Er alloy. It should be noted that during fluoride treatment, hydrogen (H_2) is produced, resulting in a porosity coating. The fluoride conversion layer is usually thin as well (16–18) μm; as a result of this, both the anti-corrosion capability and layer of coating tend to be sub-bar [9,38]. Lou et al.in 2021 [30] Studied the effect of coating magnesium fluoride on a plate of pure magnesium. We used samples with dimensions of (12×10×1) mm and immersed them in fluoric acid at a concentration of The many research used that fluoride medication is best used as a pre-treatment. Thus, more studies need to be done to develop an accurate fluoride conversion coating with the required protective properties [2,39]. This study investigates the control degradation of new material for cardiovascular applications with enhanced performance through MgF_2 coating of Mg-2Al-1Nd alloy.

2. Materials and Methods

2.1. Preparation of Alloy

The materials used in the research are pure magnesium of purity (99.9%) obtained from the mineral madencilik/turkey, pure aluminum of purity (97.9%) obtained from murat geri Dönüşüml turkey, and pure Nd of purity (98.8%) were obtained from china. The new Alloy (Mg-2%Al-1%Nd) was prepared using the investment casting method. 750 C° of mg was heated in a crucible vessel employing an electromagnetic durability combustion chamber, and the required temperature was maintained for 45 minutes; at this temperature 2%aluminum and 1% Nd were added to the melt for modifications, respectively. The molten is poured into a mold of gypsum prepared by the 3D Printer, then poured by bottom pouring arrangements into a preheated (200 C°), and placed in a device to empty air bubbles and remove them from the molten at a pressure of 1 mbar. It is poured into a protective atmosphere of SF6 (1%, v/v) and CO_2 (bal). After the solidification process, it is washed with distilled water to remove the gypsum mold and the Alloy is extracted. Then, a solution treatment was carried out for homogenizing at 350C° for a period of 2 h, followed by cooling or quenching with water at room temperature, and finally, cutting the Alloy using (wire cutting) into disc specimens with a diameter of 12mm and a height 3 mm table 1 showed the codes of the specimens in this study[11].

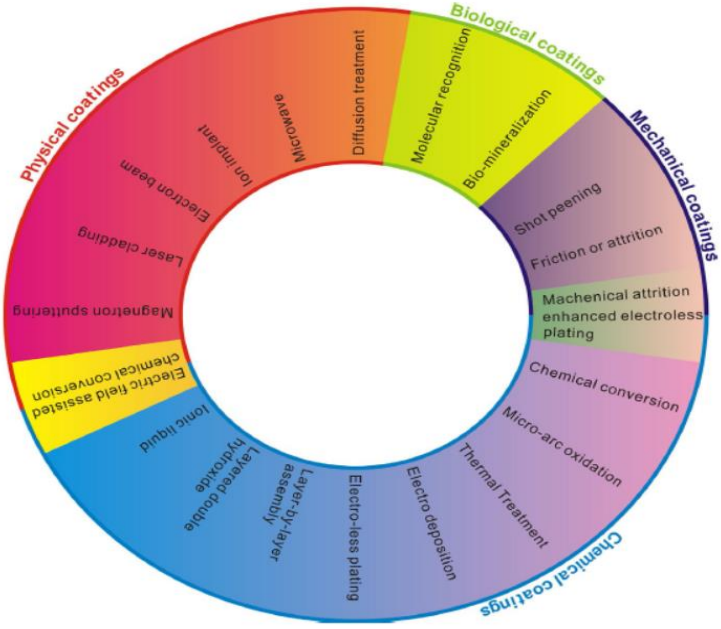

Figure 1. The diagram of coating methods of magnesium alloys [8]

2.2. Preparation of Coating

The specimen is immersed in a 20% sodium hydroxide solution that is boiling for three hours before being immersed in a diluted acid solution as the initial treatment step. The specimens were placed in closed plastic beakers and immersed in a 48% hydrofluoric acid solution at 20 ml/cm^2 for the UHF coating method, as shown in Figure 2. The beakers were then placed in an ultrasonic cleaner (SAEHAN SH-2100; ultrasonic frequency 50-60 kHz; output = 100 W) with ultrasonic at room temperature for three hours. The treated specimens were then three times washed with distilled water and dried.

Table 1. Codes of specimens in the study

Codes of specimens	Description
A	(Mg-2Al-1Nd)alloy before coating
B	(Mg-2Al-1Nd)alloy after MgF_2 coating

2.3. Characterization of Alloy

An XRD analysis was performed to determine the occurring phases. It was carried out on (Shimadzu, XRD-7000, and Japan) for all specimens before coating. The measurement settings were: Cu target at 30 mA and 40 kV, scanning speed of 2 deg /min for scanning range of 10°-80°. The microstructure of the base alloy was investigated using a scanning electron microscope (SEM) (TESCAN and Model: VEGA3SBH). Energy-dispersive spectroscopy (EDS) was used to know the existence of elements in the fabrication of the samples. Analysis was performed on the specimens to know the existence of different phases.

2.4. Coating Characterization

A scanning electron microscope (TESCAN and Model: VEGA3SBH) was used to investigate the surface layer's morphology, and X-ray diffraction (Shimadzu, XRD-7000, and Japan) was applied to identify the layer's composition (XRD). SEM was also used to analyze the layer's substructure. SEM images of the cross-sections were used to determine the samples' layer thickness. Through the use of image analysis, surface morphologies, pores, and fractures were determined.

2.4.1. Surface Roughness Measurement

Surface roughness was determined using atomic force microscopy 3D (AFM) (Digital Instruments, CSPM-AA3000), which has a distance accuracy of 1 m. Each specimen's center and edge have been measured a mean of three times.

2.4.2. Bond Strength of Coating

ISO 14916 measured the bonding strength between the fluoride treatment protection and the AN21 alloy substrate [10,40]. The diagram of the test is shown in Figure 3, in which one fluoride-coated specimen was bonded from above to another bare specimen using the chemical epoxy resin (HTE-51, Shenyang Southeast Institute of Chemical Industry), which has a binding strength of about 50 MPa. A universal tensile tester was selected for the evaluation, and an overload rate of 1 mm/min was applied from the breaks of the examination specimens; five experimental results and standard errors were determined.

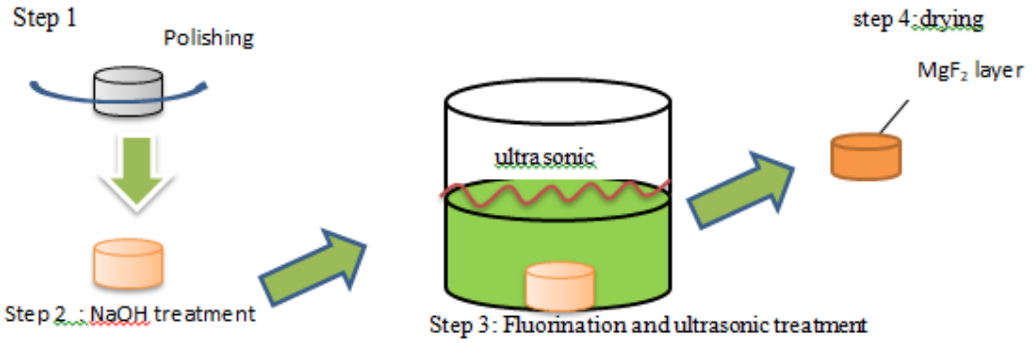

Figure 2. Preparation process of fluoride chemical conversion on Mg alloy

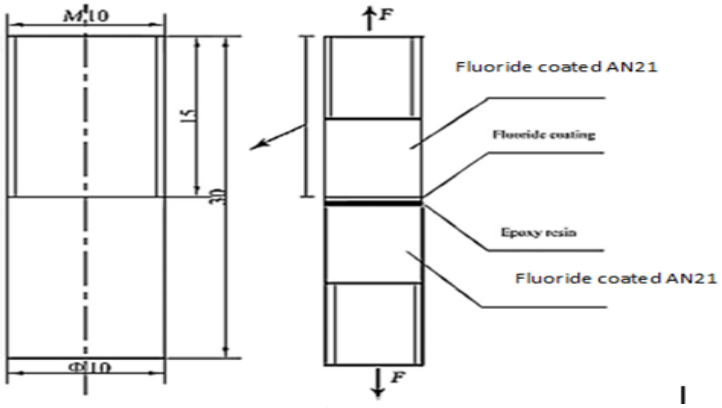

Figure 3. Sketch of bonding testing process

2.5. Potent Dynamic Polarization (PDP) test

Electrochemical tests were used to evaluate the corrosion resistance of the magnesium alloy with the fluoride film that had undergone ultrasonic treatment. Electrochemical tests were carried out at 37 C° employing a three-electrode system that included a saturated calomel reference electrode and a platinum counter electrode. The working electrode consisted of a fluoride-coated magnesium alloy that was recently ultrasonically treated. An electrochemical workstation was used to conduct the tests in phosphate buffer saline (PBS) solution of composition (in g/L) as[11]: 8.006 NaCl, 0.201 KCl, 0.240 KH_2PO_4 and 1.420 Na_2HPO_4 (pH 7.4) at 37 C° with a P.H. of 7.36 and simulated blood plasma (SBP) solution of composition (in g/L) as[12] [6.8 NaCl, 0.1$MgSO_4$, 2.2$NaHCO_3$, 0.216Na_2HPO_4, 0.026 NaH_2PO_4, 0.2 $CaCl_2$ and 0.4KCl, and deionized water] with a P.H. of 7.36 at 37 C° the sample with an exposed area of 1.13 cm^2 served as the counter electrode. Also, equation (1) is used to estimate corrosion amounts. The equation was used to define the corrosion rate based on ASTM G102 [13, 14].

$$C.R = (K\, I_{corrosion} \,.\, E.W.)/\rho \quad (1)$$

Where: C.R is the corrosion rate (mm/y), k=3.27x10^{-3} mm/g, ρ is the density of magnesium alloy, and I_{corr} is the current density E.W. = equivalent weight.

2.6. The Behavior of Degradation by Hydrogen Evolution

A different method for determining the degradation rate is to determine the volume of hydrogen evolved throughout the degradation of magnesium alloy. A funnel covers the corroded specimen, and a burette is placed inverted. The evolved hydrogen collected, thereby shifting the solution in the burette's upper part, as shown in Figure 4.

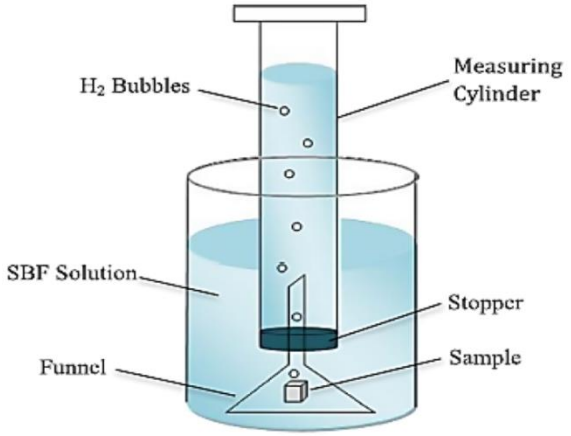

Figure 4. Schematic of hydrogen evolution method for corrosion study of Mg alloys

The soaking test was done for up to 10 days at 37 °C in PBS and simulated blood plasma fluid (SBP). To keep the immersed environment relatively steady, the solutions changed every 24 hours. The solution volume ratio to sample surface area was 100 ml/cm^2. Sample 12 mm diameter and 3 mm thickness were polished to finish on the surface. Under each circumstance, three measurements were taken. The hydrogen evolution method was employed to determine the degradation rate from the volume of hydrogen released. Figure 4 shows the setup to measure how the hydrogen evolved. The soaked specimen produced hydrogen bubbles, which were collected into a measuring vessel. The difference in elevation between the solutions in the measuring vessel can be employed to estimate how much hydrogen is there. After the immersion test, the specimens were removed from the solution, gently washed in deionized water, and dried in a cold environment. After dipping for 3 minutes in a solution of 180 g/l CrO_3 and 2g/l$AgNO_3$, the corrosion products were chemically removed [15, 16].

3. Results and Discussion

3.1. Characterization of Coating and Alloy

This work analyzed the surface morphology and chemical composition of the fluoride-treated samples. The XRD result, as shown in Figure 5, clearly indicates that the conversion coating consists of MgF_2 and MgO, representing the protective layer. Due to the coating's thinness, the magnesium alloy substrate was also identified and displayed excellent spectral resolution. According to the surface morphology of the A alloy and B alloy shown in Figure 5, the surface of the B specimen formed a dense, smooth, and dark coating with a few tiny, irregularly spaced pores. The coating's asymmetrical pores should be caused by hydrogen evolution, and throughout the fluoride conversion process, precipitations of MgF_2 and MgO particles may minimize or fill these pores.

The SEM image of the base alloy and the fluoride-treated specimen's cross-section showed the thickness of the MgF_2 layer as Figure 6. the coating layer, with a thickness of approximately 14.21 μm, adhered to the Mg-2Al-1Nd alloy substrate well shown in Figure 6, and It was also found that increasing the time of immersing the Alloy in H.F. solution increases the thickness of the layer formed [2, 17].

3.2. Surface Roughness

Both A and B alloy specimens performed roughness examinations and topographical Characterization. Figure 7 roughness assessments for the B specimen were R_{alloy} = 54.7 nm and $R_{alloy/MgF2}$ = 27.8 nm, respectively. These values showed a considerable difference between the two specimens. Figure 6 illustrates how the coating prompted the specimens' topography to change. The topography of coated specimens had a regular texture and was smoother than that of uncoated specimens. Similar-sized grooves were uniformly dispersed throughout the topography; these results agree with the references. The coating layer makes the surface less rough, reducing the pitting that causes pitting corrosion. Thus, this layer protects the Alloy from corrosion for some time [18, 19,31].

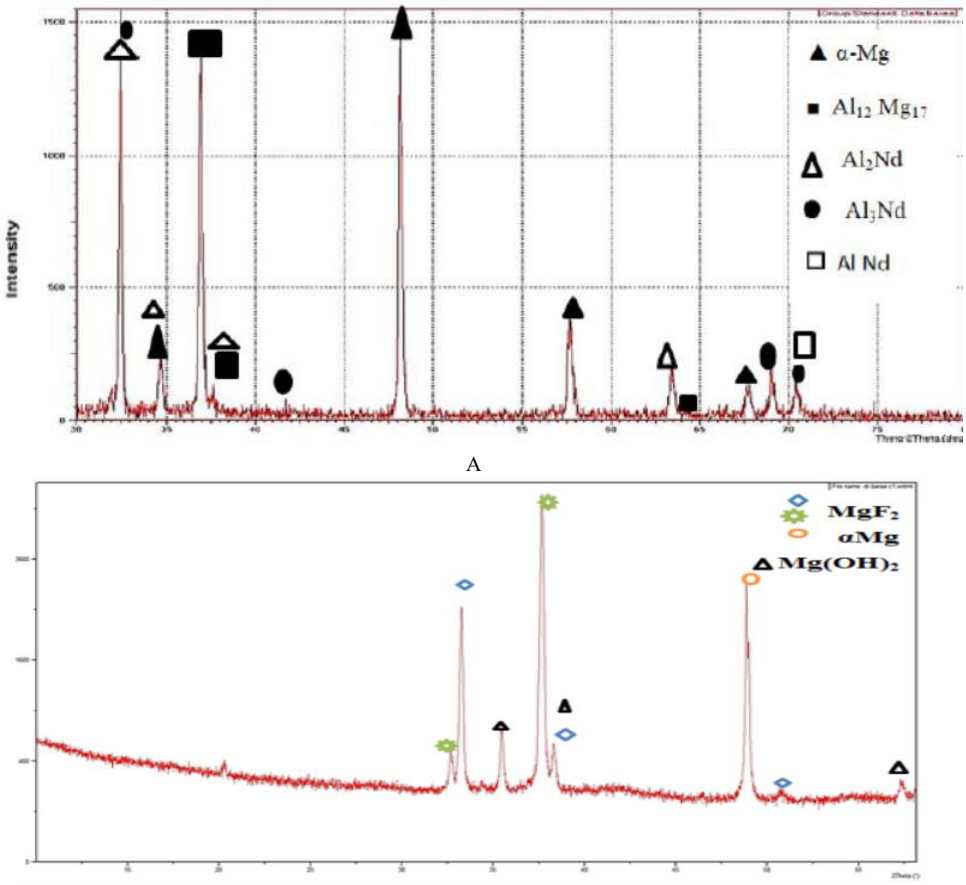

Figure 5. TF-XRD Pattern of a) annealed for Mg-2Al-1Nd alloy and b) alloy with coated

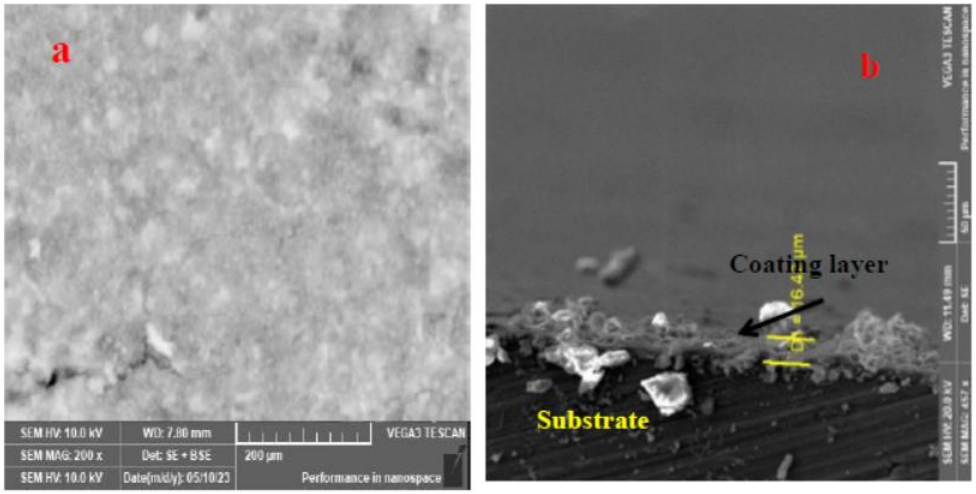

Figure 6. Surface morphology of a) AN21surface coated MgF_2 , b)cross section view of AN21alloy coated MgF_2

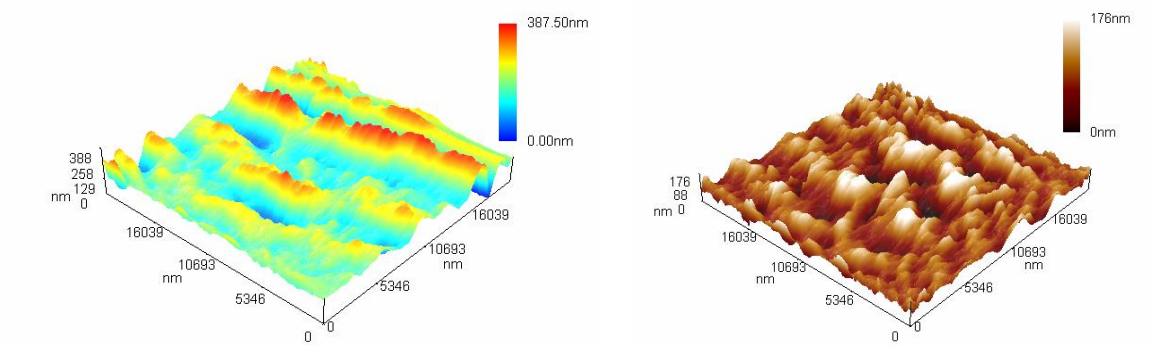

Figure 7. AFM analysis performed on Alloy: 3D images of A alloy (a) and B alloy (b)

3.3. Bonding Strength of Coating

According to the bond strength test results, the average bond strength of the substrate and fluoride coating is 50 MPa. One of the test curves is shown in Figure 6; the breakage in the epoxy resin layer occurs because the strength of the resin is lower than the degree of bonding between the fluoride coating and the alloy substrate, although the fluoride coating on the specimen after testing continues to keep its first contact with the base. Therefore, it can be assumed that the 50 MPa strength determined in the present investigation should be epoxy resin strength and that the bonding strength between the fluoride coating and alloy substrate should be greater than 50 MPa. Naturally, one of the most significant characteristics of a coating on materials is its bonding strength. It is an important part of the coating that is especially employed in biomaterials. Conforming to ASTM 1147-F, a coating on surgical implants has to have a minimum bonding strength of 22 MPa [20]. Although an accurate bonding strength measurement was not quantified, all tested coatings in the present investigation demonstrated strong bonding strengths. The mean bonding strength between the fluoride coating and alloy substrate was more than 50 MPa and satisfied the standards required by medical implants. The mechanical locking and the chemical bonding formed on the coating substrate through the coating development operation should be the two reasons for the strong connection between the fluoride coating and the alloy base [2,32], as shown in Figure 8.

3.4. Potent Dynamic Polarization (PDP) Test

The UHF-coated alloys showed significantly elevated OCP values after one hour; the standard PDP curves for both the uncoated and coated alloys can be seen in Figure 9(a); the anodic curves indicate the dissolution of magnesium, whereas the cathode polarization curves represent the evolution of cathode hydrogen through water reduction. The increased corrosion rate is shown by the increased density of corrosion currents and lower corrosion potential [21,30]. The anodic and cathodic sections in the three specimens vary significantly from one another, depending on Tafel plots of corrosion potential and current density of corrosion for the uncoated and UHF-coated alloys. It can be observed that the specimen with UHF coating had significantly greater resistance than did the untreated and bare specimens, which indicates that fluoride coating with ultrasonic treatment significantly improves corrosion resistance. The test results are shown in Figure 9 and Table 2, which illustrate the improvement of corrosion resistance of Alloy with an MgF_2 coating layer in different solutions. Also, the corrosion rate of the specimens was calculated by Equation 1.

From the table above, we note that the age of the Alloy after the coating has increased significantly in physiological solutions, and this is due to the presence of a layer of magnesium fluoride that protects the surface of the Alloy for a temporary period, and this is consistent with using magnesium alloys in the field of surgery.

3.5. Degradation Behavior by Hydrogen Evolution

For soak duration of (1-240) h, the mean degradation rate (ml/y) is determined as 4.176 ml/y for B alloy in SBP solution and 2.51 ml/y for B alloy in PBS using the formula 2.088ml/y , as Figure 10 shows that degradation of B alloy in plasma is apparent.

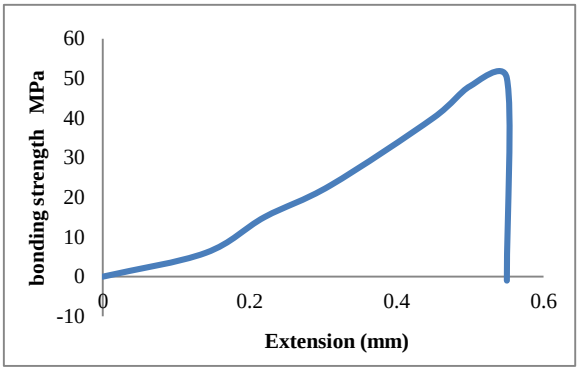

Figure 8. The bonding strength between the alloy and coating layer

Table 2. Improve shelf life for A and B alloys in physiological solutions.

Cod of Sample	PBS			SBP		
	$I_{corrosion}$ μA	$E_{corrosion}$ mV	C.R (mm/y)	$I_{corrosion}$ μA	$E_{corrosion}$ mV	C.R (mm/y)
A	826.7	-1478.2	17.07	163.37	-1342	3.37
B	74.91	-1510.1	1.55	30.16	-1450	0.62

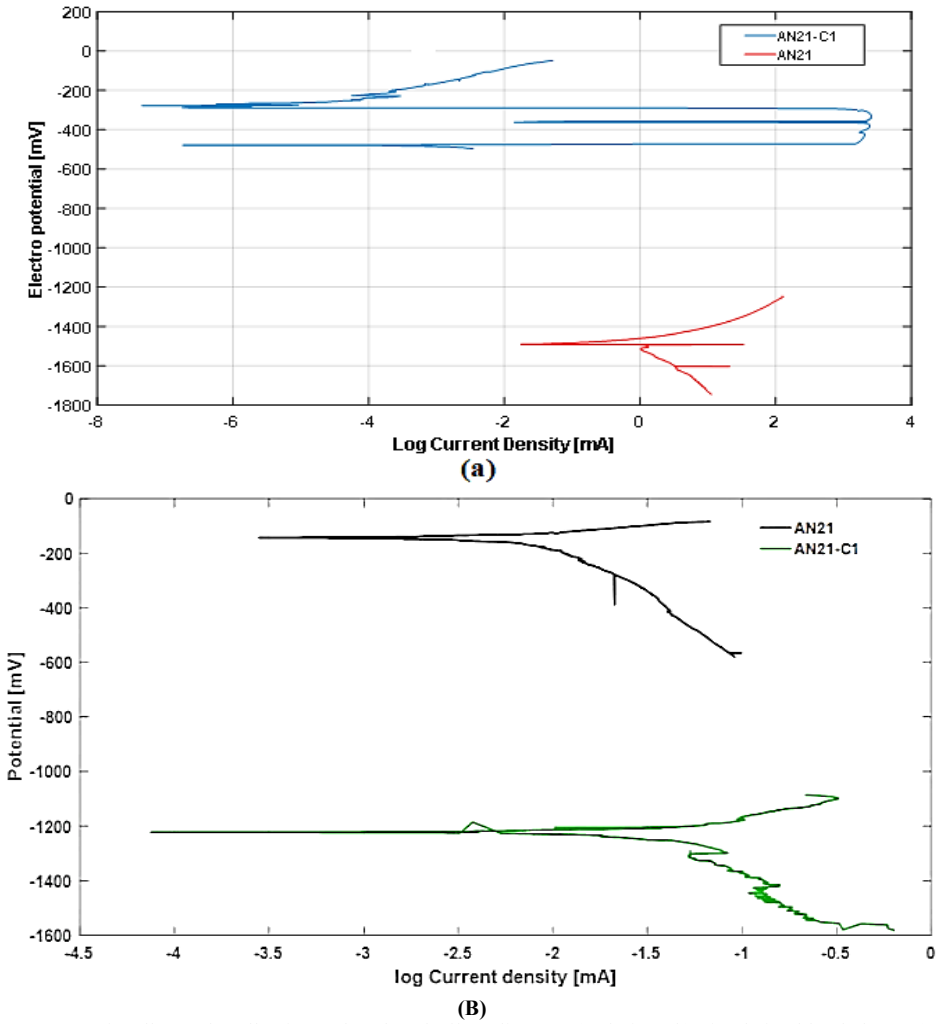

Figure 9. PDP curves of A alloy and B alloy in (a)Phosphate buffer saline(PBS)solution, (b) Simulation blood plasma (SBP) solution

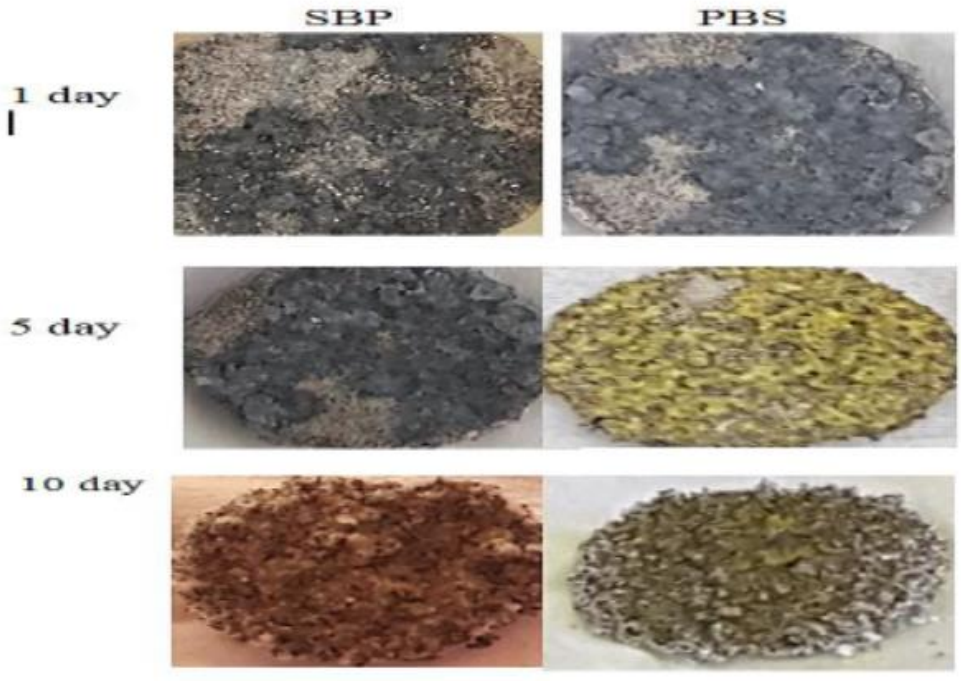

Figure 10. Photo image shown the degradation stages of Alloy for time (1-10) day

From the data in Figure 11, the specimen's surface remained smooth for 3 days, showing relatively uniform degradation. As time passed, the degradation increased almost linearly due to the in vitro soaking results; MgF_2 layer development on magnesium alloy protected the specimens' surfaces. The main reason for the results is the formation of a protective layer of magnesium fluoride on the surface of the specimens, which reduces the rate of hydrogen evolution. After some time, the protective layer is destroyed, and from it, the rate of dissolution increases, even though the degradation rate for the specimens immersed was much lower in (SBP and PBS) solutions [22, 23],[24,29]. The simulation blood plasma solution includes sodium hydrogen carbonate buffer, and its inclusion increases the reaction that takes place [5, 6]. Therefore, the dissolution rate is higher than the Phosphate buffer saline solution. As a consequence, the rate of hydrogen evolution varies from one solution to another for the same sample; the degradation rate of A and B alloy is shown in Figure 11.

4. Conclusion

Before and during a fluoride chemical conversion coating, Mg-2Al-1Nd alloy was investigated. Hydrogen evolution methods were employed to compute the degradation rate of the base alloy to reduce the degradation rate. This study's conclusions were as follows:

- Investment casting is an effective method of manufacturing new magnesium alloy; also, adding the neodymium(Nd) to Mg-Al alloy is essential in enhancing the mechanical properties and corrosion behavior.
- Ultrasonic Chemical conversion coating is one of the simplest and most successful methods for coating and protecting magnesium alloys. The MgF_2 layer can be formed to improve the surface properties and control the degradation rate.
- Applying MgF_2 layer coating improves the surface properties of AN21annealed Alloy, as the surface roughness increases while lowering the thickness of the coating, which results in good adhesion and better protection for the surface of the Alloy.

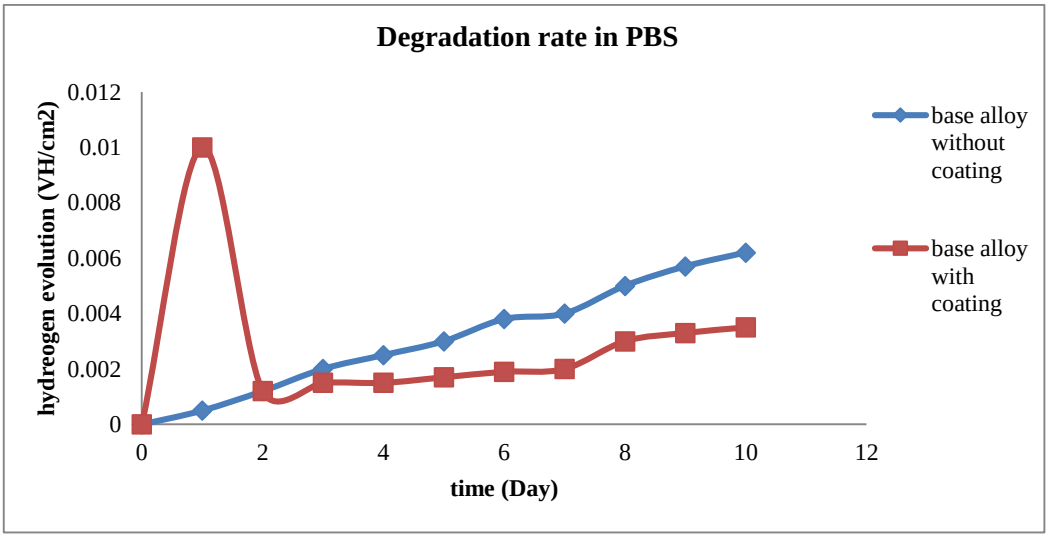

(a)

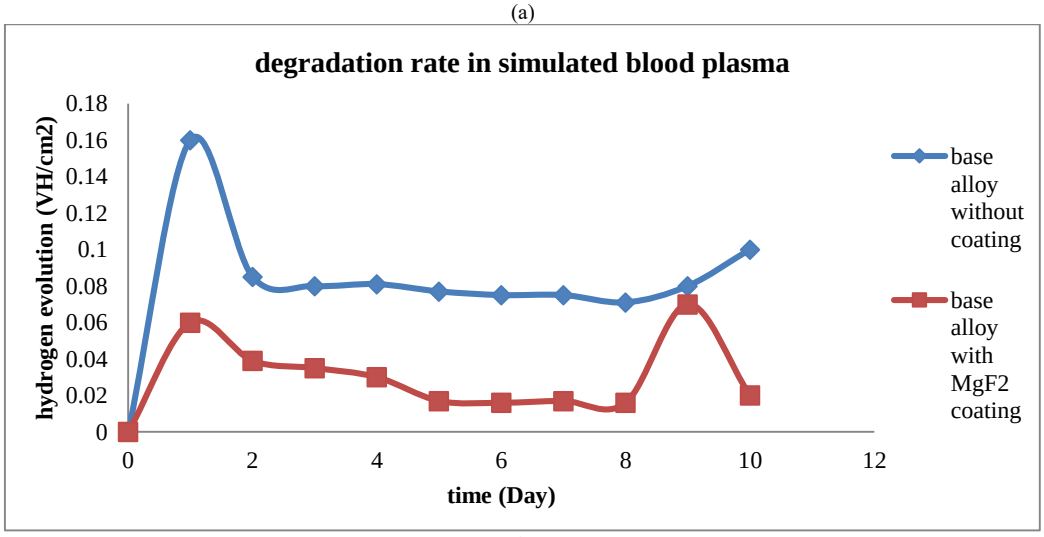

(b)

Figure 11. The degradation rate for A and B alloy during the ten-day Immersion test in (a) Phosphate buffer saline and (b) Simulated blood plasma

Conflicts of Interest

The authors declare no conflict of interest.

Author Contributions

The first and second authors have done the paper conceptualization, methodology, software, validation, formal analysis, resources, data curation, writing—original draft preparation, review and editing, visualization, supervision, project administration, and funding.

Reference

[1] Sun, J., Jin, S., Zhao, B. C., Cai, H., Sun, L., Xuan, X., ... & Jiang, H. B. "Enhanced corrosion resistance of biodegradable Mg alloys via ultrasonically treated fluoride coating". Surface Topography: Metrology and Properties, 7(2), 025009, (2019).

[2] T. Yan, L. Tan, B. Zhang, and K. Yang, "Fluoride conversion coating on biodegradable AZ31B magnesium alloy," Journal of Materials Science & Technology, vol. 30, no. 7, pp. 666-674, 2014.

[3] J. Barajas, J. Joya, K. Durán, C. Hernández-Barrios, A. Coy, and F. Viejo, "Relationship between microstructure and formation-biodegradation mechanism of fluoride conversion coatings synthesised on the AZ31 magnesium alloy," Surface and Coatings Technology, vol. 374, pp. 424-436, 2019.

[4] S. Gambaro "Characterization of a Magnesium Fluoride Conversion Coating on Mg-2Y-1Mn-1Zn Screws for Biomedical Applications," Materials, vol. 15, no. 22, p. 8245, 2022.

[5] M. Schinhammer, J. Hofstetter, C. Wegmann, F. Moszner, J. F. Löffler, and P. J. Uggowitzer, "On the immersion testing of degradable implant materials in simulated body fluid: active pH regulation using CO2," Advanced Engineering Materials, vol. 15, no. 6, pp. 434-441, 2013.

[6] T. Kraus, S. F. Fischerauer, A. C. Hänzi, P. J. Uggowitzer, J. F. Löffler, and A. M. Weinberg, "Magnesium alloys for temporary implants in osteosynthesis: in vivo studies of their degradation and interaction with bone," Acta biomaterialia, vol. 8, no. 3, pp. 1230-1238, 2012.

[7] Y. Han "Facile synthesis of morphology and size-controlled zirconium metal–organic framework UiO-66: the role of hydrofluoric acid in crystallization," CrystEngComm, vol. 17, no. 33, pp. 6434-6440, 2015.

[8] H. Hermawan and H. Hermawan, "Biodegradable metals for cardiovascular applications," Biodegradable metals: from concept to applications, pp. 23-37, 2012.

[9] S. Fintová ,"Degradation of unconventional fluoride conversion coating on AZ61 magnesium alloy in SBF solution," Surface and Coatings Technology, vol. 380, p. 125012, 2019.

[10] J. Lou, "Effects of MgF2 coating on the biodegradation and biological properties of magnesium," Surface and Coatings Technology, vol. 422, p. 127552, 2021.

[11] Al Khaqani, Baraa H., and Nawal Mohammed Dawood. "Investigate the Metallurgical, Degradation Behaviour, and Mechanical Characteristics of Mg-2Al-1Nd: Novel Magnesium Alloy." Advances in Science and Technology Research Journal 17.5 (2023): 302-312.

[12] S. Mishra, A. Chaubey, and A. Mandal, "Effect of heat treatment on the microstructure of Mg-4Al-Nd alloys," Technologies, vol. 5, no. 2, p. 23, 2017.

[13] G. Astm, "Standard practice for calculation of corrosion rates and related information from electrochemical measurements," G102-89, 2004.

[14] S. Shinde and S. Sampath, "A Critical Analysis of the Tensile Adhesion Test for Thermally Sprayed Coatings," Journal of Thermal Spray Technology, vol. 31, no. 8, pp. 2247-2279, 2022.

[15] A. Jana, M. Das, and V. K. Balla, "In vitro and in vivo degradation assessment and preventive measures of biodegradable Mg alloys for biomedical applications," Journal of Biomedical Materials Research Part A, vol. 110, no. 2, pp. 462-487, 2022.

[16] Y. Lu, A. Bradshaw, Y.-L. Chiu, and I. Jones, "Effects of secondary phase and grain size on the corrosion of biodegradable Mg–Zn–Ca alloys," Materials Science and Engineering: C, vol. 48, pp. 480-486, 2015.

[17] W. Peng, Y. Chen, H. Fan, S. Chen, H. Wang, and X. Song, "A Novel PLLA/MgF2 Coating on Mg Alloy by Ultrasonic Atomization Spraying for Controlling Degradation and Improving Biocompatibility," Materials, vol. 16, no. 2, p. 682, 2023.

[18] X. Li, X. Liu, S. Wu, K. Yeung, Y. Zheng, and P. K. Chu, "Design of magnesium alloys with controllable degradation for biomedical implants: From bulk to surface," Acta biomaterialia, vol. 45, pp. 2-30, 2016.

[19] M. Lin, "Enhanced Bioactivity of Mg–Nd–Zn–Zr Alloy Achieved with Nanoscale MgF2 Surface for Vascular Stent Application," 2015.

[20] B. Niu, P. Shi, E. Shanshan, D. Wei, Q. Li, and Y. Chen, "Preparation and characterization of H.A. sol–gel coating on MAO coated AZ31 alloy," Surface and Coatings Technology, vol. 286, pp. 42-48, 2016.

[21] B. R. Fazal and S. Moon, "Effect of fluoride conversion coating on the corrosion resistance and adhesion of E-painted AZ31 magnesium alloy," Journal of the Korean institute of surface engineering, vol. 49, no. 5, pp. 395-400, 2016.

[22] N. I. Z. Abidin, A. D. Atrens, D. Martin, and A. Atrens, "Corrosion of high purity Mg, Mg2Zn0. 2Mn, ZE41 and AZ91 in Hank's solution at 37 C," Corrosion Science, vol. 53, no. 11, pp. 3542-3556, 2011.

[23] N. Kirkland, N. Birbilis, and M. Staiger, "Assessing the corrosion of biodegradable magnesium implants: A critical review of current methodologies and their limitations," Acta biomaterialia, vol. 8, no. 3, pp. 925-936, 2012.

[24] A. Bordbar-Khiabani, B. Yarmand, and M. Mozafari, "Enhanced corrosion resistance and in-vitro biodegradation of plasma electrolytic oxidation coatings prepared on AZ91 Mg alloy using ZnO nanoparticles-incorporated electrolyte," Surface and Coatings Technology, vol. 360, pp. 153-171, 2019.

[25] W. Ng, K. Chiu, and F. Cheng, "Effect of pH on the in vitro corrosion rate of magnesium degradable implant material," Materials Science and Engineering: C, vol. 30, no. 6, pp. 898-903, 2010.

[26] R. Tunold, H. Holtan, M.-B. Berge, A. Lasson, and R. Steen-Hansen, "The corrosion of magnesium in aqueous solution containing chloride ions," Corrosion Science, vol. 17, no. 4, pp. 353-365, 1977.

[27] E. DIN, "14916: 2017: Thermal spraying—Determination of tensile adhesive strength," International Organization for Standardization, ICS, vol. 25, pp. 20-26, 2017.

[28] F. E.-T. Heakal and A. M. Bakry, "Corrosion degradation of AXJ530 magnesium alloy in simulated pysiological fluid and its mitigation by fluoride and chitosan coatings for osteosynthetic applications," Int. J. Electrochem. Sci, vol. 13, no. 8, pp. 7724-7747, 2018.

[29] Tashtoush, G. M., T. K. Aldoss, and A. O. Al-Jabaly. "A novel magnetohydrodynamic power generation system using low-temperature liquid metal coupled with a rectangular single-phase natural circulation loop." Jordan Journal of Mechanical and Industrial Engineering, 81.1 (2024).

[30] Jeyanthi, S. "A Comparative Analysis of Flexible Polymer-Based Poly (vinylidene) Fluoride (PVDF) Films for Pressure

Sensing Applications." *Jordan Journal of Mechanical and Industrial Engineering*, 17.3 (2023).

[31] Zhang, Qian, Huang Tang, and Shihui Guo. "Calculation Method of Stiffness and Deflection of Corroded RC Beam Strengthened by Steel Plate." Jordan Journal of Mechanical and Industrial Engineering 15.1 (2021)

[32] Azad, Abdul Kalam, "Fabrication of Al-6061/SiC Nano Composite Material Through Ultrasonic Cavitation Technique and Its Analysis." Jordan Journal of Mechanical and Industrial Engineering, 17.3 (2023).

[33] Asmael, Mohammed, OtonyeTekena Fubara, and Tauqir Nasir. "Prediction of Springback Behavior of Vee Bending Process of AA5052 Aluminum Alloy Sheets Using Machine Learning." Jordan Journal of Mechanical and Industrial Engineering 17.1 (2023).

[34] Damseh, Rebhi A. "Chemically Reactive Nanofluid Flowing across Horizontal Cylinder." Jordan Journal of Mechanical and Industrial Engineering 17.1 (2023).

[35] Ekpruke, E. O., C. V. Ossia, and A. Big-Alabo. "On the Morphological and Tribological Characterization of Green Automotive Brake Pads Developed from Waste Thais Coronata Seashells." Jordan Journal of Mechanical and Industrial Engineering 17.2 (2023).

[36] Ali, Raad Mohammed Kadhim, and Sajida Lafta Ghashim. "Thermal performance analysis of heat transfer in pipe by using metal foam." Jordan Journal of Mechanical and Industrial Engineering 17.2 (2023).

[37] Nafteh, MassoumehAzizi, and Mahmoud Shahrokhi. "Improving the COPRAS Multicriteria Group Decision-Making Method for Selecting a Sustainable Supplier Using Intuitionistic and Fuzzy Type 2 Sets." Jordan Journal of Mechanical and Industrial Engineering 17.2 (2023).

[38] Sadashiva, K., and K. M. Purushothama. "Investigation on Mechanical and Morphological Characteristics of Ramie/Silk with Epoxy Hybrid Composite of Filler OMMT Nanoclay." Jordan Journal of Mechanical and Industrial Engineering 17.2 (2023).

[39] Balcha, Robson, Perumalla Janaki Ramulu, and Belay Brehane Tesfamariam. "Mechanical Behaviour Assessment of Banana Fibres Reinforced Polymeric Composite with Aluminium-Powder Filler." Jordan Journal of Mechanical and Industrial Engineering 17.2 (2023).

[40] Al-Shalabi, B., Almomani, M., Abu-Awwad, M., & Al-Ajlouni, M. "Selecting the Best Material for Hydrogen Storage Using the Analytical Hierarchical Process." Jordan Journal of Mechanical and Industrial Engineering 17.2 (2023).